J Electr Eng Technol.2015; 10(3): 1311-1318
http://dx.doi.org/10.5370/JEET.2015.10.3.1311

ISSN(Print) 1975-0102
ISSN(Online) 2093-7423

Versatile Shunt Hybrid Power Filter to Simultaneously Compensate Harmonic Currents and Reactive Power

Quoc-Nam Trinh* and Hong-Hee Lee†

Abstract – This paper introduces a novel topology and an effective control strategy for a shunt hybrid power filter (SHPF) to simultaneously compensate harmonic currents and reactive power. The proposed SHPF topology is composed of an *LC* passive filter tuned to the 7th harmonic frequency and a small-rated active filter connected in parallel with the inductor L_{pf} of the *LC* passive filter. Together with the SHPF topology, we also propose a control strategy, which consists of a proportional-integral (PI) controller for DC-link voltage regulation and a PI plus repetitive current controller, in order to compensate both the harmonic current and the reactive power without the need for additional hardware. Thanks to the effectiveness of the proposed control scheme, the supply current is sufficiently compensated to be sinusoidal and in-phase with the supply voltage, regardless of the distorted and phase lagging of the load current. The effectiveness of the proposed SHPF topology and control strategy is verified by simulated and experimental results.

Keywords: Hybrid shunt power filter, Harmonic current, Reactive power

1. Introduction

Nowadays, the use of power electronics devices such as diode rectifiers, adjustable speed drives, power supplies, and large air condition systems, are becoming increasingly popular. These devices are nonlinear loads that generate harmonic currents and reactive power in distribution power systems. High current harmonic distortion leads to various problems in both distribution systems and consumer products, including equipment and transformer overheating, malfunction of protection devices, reducing power system efficiency. High reactive power consumed by loads may increase power losses and lower network stability. Therefore, compensation for harmonic current and reactive power is a mandatory requirement for system operators and end users.

Traditionally, *LC* passive filters have been used to suppress current harmonics in distribution power systems due to their low cost and simplicity. However, they have many problems, such as low dynamic performance and resonance problems, and their filtering characteristics can be easily affected by system parameters [1]. Active power filters (APFs) have been developed to overcome the disadvantages of *LC* passive filters [2-5]. APFs can offer flexible control functionalities, but their high initial and operational costs are the main barriers that limit their application in practice.

To provide a cost-effective solution for harmonic current compensation in power distribution systems, various shunt hybrid power filter (SHPF) topologies composed of active and passive parts have been introduced [6-15]. Among these approaches, SHPFs with tuned passive filters connected in series with a small-rated active filter are popularly utilized for harmonic current compensation. The main advantages of these SHPF topologies are the low operating DC-link voltage, reduced number of passive components, and small size and volume thanks to the absence of coupling trans-formers [6-9]. Unfortunately, due to the series connection of passive and active parts, this type of SHPF can supply only a fixed amount of reactive power; it is unable to perform a dynamic reactive power compensation function when the load changes. To overcome this limitation, several novel SHPF topologies have been proposed to simultaneously take into account the harmonic currents and the reactive power [10-14]. In [10-12], additional passive components, such as capacitors, inductors, or coupling transformers, were inserted into the typical SHPF to improve harmonic current and reactive power compensation capability. However, these approaches required additional hardware, which degraded the cost-effective advantage of the SHPF. In [13], an enhanced control algorithm for SHPF was proposed to compensate harmonic current and reactive power. The suggested control method was able to fulfill the control target, but the control algorithm was very complex with many control stages. A combination of an SHPF and a thyristor-controlled reactor was introduced to perform both harmonic current and reactive power compensation functions [14]. The control method was simple and effective, but the demand of extra hardware was again a drawback of this method.

† Corresponding Author: School of Electrical Engineering, University of Ulsan, Korea. (hhlee@mail.ulsan.ac.kr)
* Energy Research Institute, Nanyang Technological University, Singapore. (tqnam@ntu.edu.sg)
Received: November 23, 2014; Accepted: December 29, 2014

To overcome the limitations of previous SHPF topologies, this paper proposes a new SHPF topology and an effective control strategy, introduced succinctly in [15], to simultaneously achieve the harmonic current and reactive power compensation. The proposed SHPF is composed of an *LC* passive filter tuned at the 7th harmonic frequency and a small-rated APF, where the APF is connected in parallel with the inductor L_{pf} of the *LC* passive filter. In the proposed configuration, the control strategy is developed to compensate both the harmonic current and the reactive power without the need for additional hardware. The proposed algorithm applied to the SHPF consists of a proportional-integral (PI) controller for DC-link voltage regulation and a PI plus repetitive current controller for harmonic current and reactive power compensation. The supply current after compensation is almost sinusoidal with very low THD and is in-phase with the supply voltage with an almost unity power factor (PF). In this paper, we present the analysis and design of the proposed SHPF topology and the proposed control strategy in detail. The effectiveness of the proposed SHPF topology and control strategy is verified through comparative simulations and experimental results.

2. Proposed Control Strategy for SHPF

2.1 Configuration of a typical SHPF

Fig. 1 shows the configuration of a typical SHPF topology. The SHPF is composed of an *LC* passive filter connecting in series with a small-rated APF. This type of SHPF is popularly used because it requires a small number of passive components and it can lessen the DC-link voltage of the APF, which results in a lower system cost for the SHPF system. However, due to the series connection of the passive and active parts, the APF can only supply a fixed amount of reactive power, so dynamic compensation of reactive power with load changes is unable to be achieved.

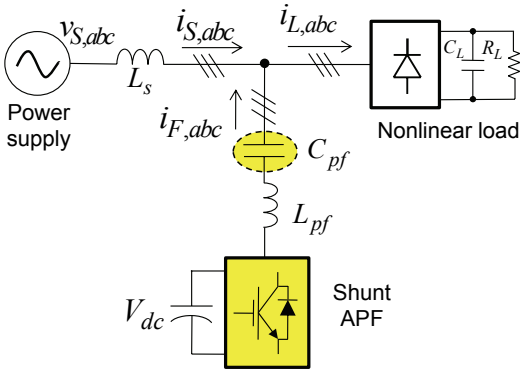

Fig. 1. Typical shunt hybrid power filter

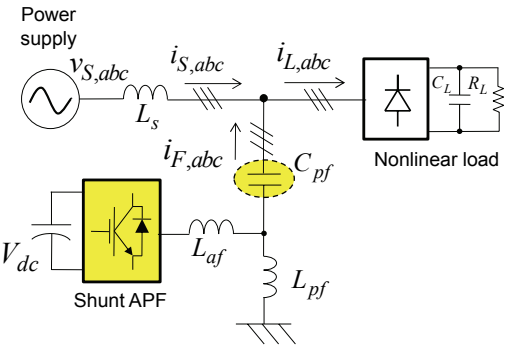

Fig. 2. The proposed shunt hybrid power filter

2.2 The proposed SHPF

To overcome the limitation to reactive power compensation of the typical SHPF configuration, shown in Fig. 1, this paper develops a new SHPF topology, shown in Fig. 2. In this SHPF topology, the active part is connected in parallel with the inductor L_{pf}. Thanks to the parallel connection of passive and active parts, dynamic compensation for the reactive power of the SHPF can be achieved. In addition, low DC-link voltage of the APF is still realized because of the APF connected with the system through the capacitor C_{pf}.

3. Analysis and Control of the Proposed SHPF

3.1 Equivalent circuit of proposed SHPF

In the equivalent model of the proposed SHPF, illustrated in Fig. 3, the APF is considered as a controllable voltage source v_{APF}, and the load is regarded as a current source i_L. From Fig. 3, the voltage and current equations of the system are determined as

$$\begin{cases} i_S = i_L - i_F \\ i_F = i_{AF} + i_{PF} \\ v_1 = v_2 + i_F X_{C_{pf}} \\ v_2 = v_{APF} + i_{AF} X_{L_{af}} \\ v_{APF} = K_p i_{Sh} \end{cases} . \quad (1)$$

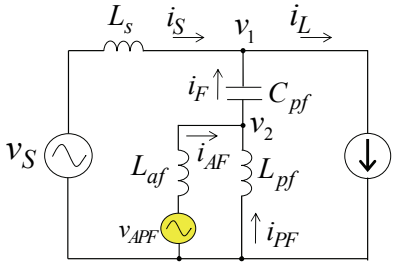

Fig. 3. Control strategy for proposed SHPF

From (1), the harmonic components in the supply current can be determined from the load current and supply voltage as

$$i_S(h) = f(i_L(h)) + f(v_S(h)), \tag{2}$$

where

$$\begin{cases} f(i_L(h)) = -i_L(h)\dfrac{Z_{HPF}}{Z_{HPF} + K_p\dfrac{L_{pf}}{L_{pf}+L_{af}} + Z_S} \\ f(v_S(h)) = -v_S(h)\dfrac{Z_{HPF}}{Z_{HPF} + K_p\dfrac{L_{pf}}{L_{pf}+L_{af}} + Z_S} \end{cases}, \tag{3}$$

and $Z_{HPF} = X_{Cpf} + X_{Lpf} // X_{Laf}$.

From (2) and (3), assuming that the supply voltage harmonics are very small, the supply current waveform mainly depends on the parameters of the passive filters and the controller function of the APF, K_p. As a consequence, to compensate the harmonic components in the supply current, the designs of the passive components and the controller play equally vital roles.

3.2 Design of passive components

In the SHPF, C_{pf} and L_{pf} together operate as a passive filter to sink a specific, e.g., the 5th or 7th, harmonic current generated by the nonlinear loads. In this paper, C_{pf} and L_{pf} are tuned to absorb the 7th-order harmonic current (h_1=7). The reason we select the 7th harmonic is that the volume and cost of C_{pf} and L_{pf} are lower for the 7th than for the 5th harmonic frequency [6].

$$\omega_{res} = h_1(2\pi f_s) = \frac{1}{\sqrt{L_{pf}C_{pf}}}, \tag{4}$$

where f_s denotes the fundamental frequency of the system, which is 60 Hz in this paper.

In addition, C_{pf} can also supply a part of the reactive power demanded by the load, which is calculated as

$$Q_c = (V_{l-l})^2(2\pi f_s)C_{pf}, \tag{5}$$

where $V_{l\text{-}l(RMS)}$=208 V is the RMS value of the line-to-line voltage in this paper.

From (5), we can see that a higher value of C_{pf} will compensate a larger amount of reactive power. However, since reactive power can also be compensated by an active filter, in order to reduce the volume of capacitor C_{pf}, we choose C_{pf} to be only 50% of the base capacitance of the system C_b [6], where C_b is defined as

$$Z_b = \frac{(V_{l-l})^2}{P_L}$$

$$C_b = \frac{1}{(2\pi f_s)Z_b}, \tag{6}$$

where P_L = 5 kW is the rating power of load.

Therefore,

$$C_f = C_b/2 = 76.63\ \mu F. \tag{7}$$

The closest commercial capacitance is chosen, i.e., $C_{pf} = 75\,\mu F$.

From (4), we can obtain L_{pf} as

$$L_{pf} = 1/\omega_{res}^2 C_{pf} = 1.875\,mH. \tag{8}$$

3.3 Control strategy for proposed SHPF

In the previous section, the passive filter was designed to compensate the 7th harmonic and a fixed amount of the reactive power demanded by the load. The other harmonic components and the remaining reactive power should be compensated by the APF. The proposed control strategy, shown in Fig. 4, consists of four parts: DC-link voltage control, harmonic compensation, reactive power compensation, and current regulation. In this case, the SHPF is operated autonomously without an external power supply. Therefore, a DC-link voltage controller developed based on a proportional-integral (PI) controller is used to regulate the DC-link voltage of the APF. The output of this control loop is the reference current in the d-axis (i^*_{AFd1}). This reference current is added to the reference current of the harmonic compensation scheme. Meanwhile, in the harmonic compensation block, the three-phase supply current is measured and transformed to the synchronous (*d-q*) reference frame through an *abc-dq* transformation, as follows

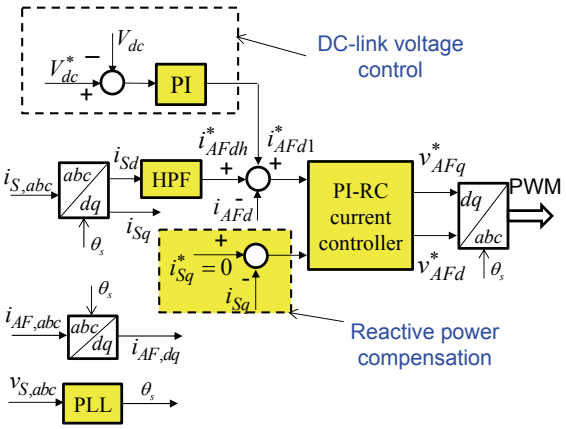

Fig. 4. Control strategy for proposed SHPF

$$\begin{bmatrix} i_{Sd} \\ i_{Sq} \end{bmatrix} = \sqrt{\frac{2}{3}} \begin{bmatrix} \cos(\theta_s) & \cos(\theta_s - \frac{2\pi}{3}) & \cos(\theta_s + \frac{2\pi}{3}) \\ -\sin(\theta_s) & -\sin(\theta_s - \frac{2\pi}{3}) & -\sin(\theta_s + \frac{2\pi}{3}) \end{bmatrix} \begin{bmatrix} i_{Sa} \\ i_{Sb} \\ i_{Sc} \end{bmatrix} \quad (9)$$

.

Then, the high-pass filter (HPF) given in (10) is applied to extract the harmonic components from the supply current, which becomes the reference current signal i^*_{AFdh} .

$$G_{HPF}(s) = \frac{s^2}{s^2 + 2\xi\omega_p s + \omega_p^2}, \quad (10)$$

where $\omega_p = 2\pi \cdot 10$ (rad/s) is the selected passing frequency of the HPF.

Reactive power compensation can be achieved easily by using a reference current along the q-axis of $i^*_{Sq} = 0$. After finding the reference current for the current controller, the measured supply current is compared with its reference value, and the error is fed into the PI-repetitive controller (RC) to generate the control signal for the APF. The transfer functions of the RC in continuous and discrete time are

$$\begin{aligned} G_{RC}(s) &= \frac{K_r Q(s) e^{-sT_d}}{1 - Q(s) e^{-sT_d}} \\ G_{RC}(z) &= \frac{K_r Q(z) z^{-N} z^k}{1 - Q(z) z^{-N}} \end{aligned}, \quad (11)$$

where $N = T_d / T_s$ is the number of delay samples, which is an integer, T_s is the sampling period, $Q(z)$ is a filter transfer function, K_r is the RC controller gain, and z^k is a phase lead term to compensate the phase lag caused by plant $G_p(z)$.

3.4 Design of repetitive current controller

To design the RC in (11), three components are considered: the filter $Q(z)$, the phase lead term z^k, and the RC controller gain K_r. First, we have to determine the filter $Q(z)$ that is used to improve the system stability by reducing the peak gain of the RC in the high-frequency range. Then, the phase lead term z^k is designed to compensate the phase lag caused by the control plant to achieve better harmonic compensation performance of the RC. Finally, the RC's controller gain K_r is chosen based on the system stability condition in (14).

3.4.1 Selection of the filter Q(z):

$Q(z)$ is used to improve the system stability by reducing the peak gain of the RC in the high-frequency range. There are two popular methods used in previous studies to employ $Q(z)$: a closed unity gain $Q(z)$=0.95 and a zero-phase LPF $Q(z) = (z + 2 + z^{-1})/4$ [16], [17]. In this study, these two types of $Q(z)$ are also adopted, and the Bode diagrams of the RC for each $Q(z)$ are plotted in Fig. 5 in order to determine a suitable $Q(z)$ for the RC. In Fig. 5, when $Q(z)$=0.95, the RC provides high gain over the entire frequency range, so the system becomes unstable due to the high gain in the high-frequency region. In contrast, for $Q(z) = (z + 2 + z^{-1})/4$, the gain of the RC is high at low-order harmonics, but it reduces to significantly less than 0 dB in the high-frequency range (above 2 kHz). It is well-known that a low peak gain in the high-frequency range can ensure a robust system. Furthermore, in contrast to the typical first-order LPF, a zero-phase LPF does not shift to the original position of the RC peak gain. Therefore, the use of this zero-phase LPF does not have an impact on the RC accuracy; thus, we choose $Q(z) = (z + 2 + z^{-1})/4$.

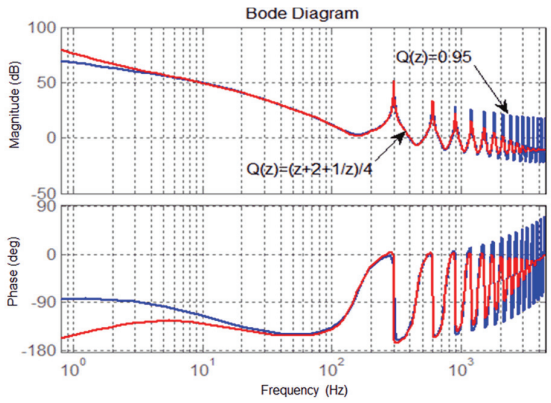

Fig. 5. Bode diagram of the PI-RC controller with $Q(z) = 0.95$ and $Q(z) = (z + 2 + z^{-1})/4$.

3.4.2 Determination of the phase-lead term z^k:

Because the control plant $G_p(z)$ commonly acts as a low-pass filter, which introduces some phase lag, a phase-lead term z^k is needed to compensate the phase lag of $G_p(z)$, and k is selected to minimize the phase displacement of , where $G_p(z)$ is the inductor L_{af}.

$$G_p(z) = \frac{T_s}{(L_{af} + T_s R_{af}) - L_{af} z^{-1}}. \quad (12)$$

Fig. 6 shows the Bode diagram of $G_p(z)z^k$ with respect to different values of k. From Fig. 6, we select k=5 because

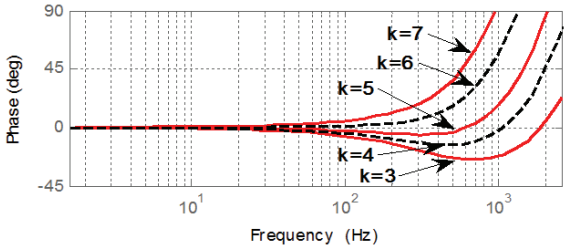

Fig. 6. Phase-lag compensation for different values of k.

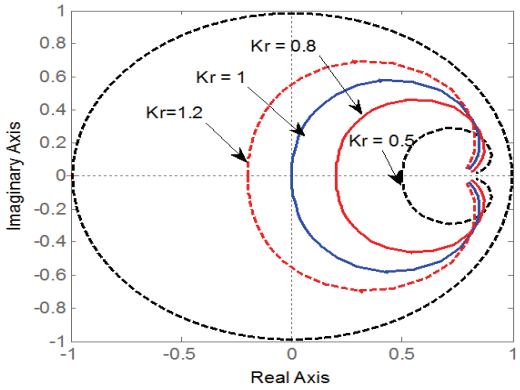

Fig. 7. Loci of the vector $H(e^{j\omega T_s})$

it provides the minimum phase displacement near the dominant harmonics, such as the 5th, 7th, 11th, and 13th, and system stability is guaranteed up to the 37th harmonic component at a frequency of 2.22 kHz. Furthermore, to remove the effect of delay time due to digital control in the experimental implementation, k=6 is used.

3.4.3 Determination of the controller gain K_r:

To investigate the stability condition of the RC and to determine the controller gain K_r, the tracking error of the RC with respect to the reference value is defined as

$$E(z) = \frac{[1-Q(z)z^{-N}][1-G_p(z)]}{1-z^{-N}[Q(z)-K_r z^k G_p(z)]} R(z). \quad (13)$$

Let $H(z) = Q(z) - K_r z^k G_p(z)$. Based on the small gain theorem [17], the repetitive control system is sufficiently stable if the vector $H(e^{j\omega T_s})$ locates within the unity circle. Consequently, the stability condition of the repetitive control system is given as

$$\left|H(e^{j\omega T_s})\right| < 1, \quad (14)$$

$\omega \in [0, \pi / T_s]$, where π / T_s is the Nyquist frequency.

The controller gain K_r is determined to satisfy the stability condition given in (14). To select the proper value for K_r, the loci of the vector $H(e^{j\omega T_s})$ is shown in Fig. 7 with respect to different values of K_r. It can be observed that the vector $H(e^{j\omega T_s})$ is located inside the unity circle; i.e., the system is stable if K_r is less than 1.2. In fact, a large K_r offers a better steady-state performance as well as faster response but limits the stability margin of the system at the same time. Therefore, to guarantee a sufficient stability margin, we select K_r=0.8.

4. Simulation results

To verify the effectiveness of the proposed control strategy for the SHPF, a simulation model is built in the PSIM software. The system parameters are given in Table 1. In the simulation system, the load consists of a three-phase diode rectifier (nonlinear load) and a three-phase *RL* (linear load) with total harmonic distortion (THD) and power factor (PF) of the load current of about 17.4% and 0.746, respectively. The SHPF is installed to compensate the harmonic current and the reactive power, and so the supply current can be compensated so that it is sinusoidal and in-phase with the supply voltage.

Table 1. System parameters

Supply voltage and frequency	$V_{l-l(rms)} = 208\text{V},\ f_s = 60\,\text{Hz}$
Passive filters	$C_{pf} = 75\mu F, L_{pf} = 1.9mH$
APF parameters	$V_{dc}^* = 80\text{V}, C_{dc} = 2200\mu\text{F},$ $L_{af} = 2\text{mH}, R_{af} = 0.1\text{mH}$
Three-phase diode rectifier parameters	$C_L = 2200\mu F, R_{L\min} = 20\Omega,$ $R_{L\max} = 40\Omega$
RL linear load	$R = 30\Omega, L = 50mH$
Sampling and switching frequency	$f_{sw} = 9\,\text{kHz}$

Fig. 8 shows the simulation results of the traditional SHPF topology using the control strategy introduced in [6], where reactive power compensation is not considered. It can be observed in Fig. 8 that the supply current can be compensated for such that it is almost sinusoidal despite the distorted load current waveform. The THD of the supply current after compensation is about 3.27%. However, because the reactive power is not considered and compensated for, the supply current is lagged compared to the supply voltage with a power factor (PF) of 0.85. The THD of the supply current is greatly reduced, but its PF cannot be significantly improved because the reactive power is not taken into account in the conventional control system.

These limitations of the traditional control method can be overcome by the proposed SHPF topology and control strategy, as demonstrated by the simulation results shown

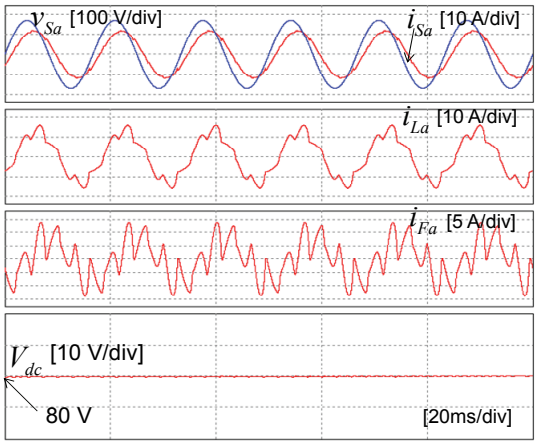

Fig. 8. Simulation results of traditional SHPF without reactive power compensation

in Fig. 9. In Fig. 9, the supply current after compensation is almost sinusoidal and is in-phase with the supply voltage. The THD and PF of the supply current after compensation are about 1.47% and 0.997, respectively. These results verify the feasibility of the proposed SHPF scheme for harmonic current and reactive power compensation.

In addition to a good steady-state performance, a dynamic response of the SHPF to load changes is also an important factor. To assess the dynamic performance of the SHPF, simulation results of the supply current under load changing is shown in Fig. 10. As shown in Fig. 10(a), when the load current has a step increase, the SHPF quickly responds to compensate the load change and maintain the supply current as sinusoidal and in-phase with the supply voltage. During a load increase, the DC-link voltage suffers a small reduction, but it restores to the initial value within a short period of time. A similar dynamic performance of the SHPF is shown in Fig. 10(b) when the load current is reduced. Finally, we can conclude that the supply current is effectively compensated to be sinusoidal and in-phase with the supply voltage regardless of the load current conditions.

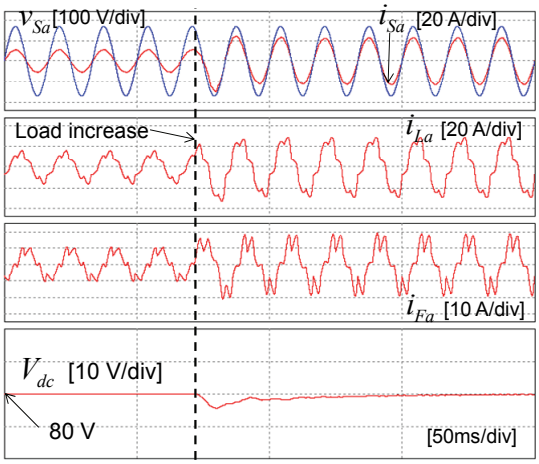

(a)

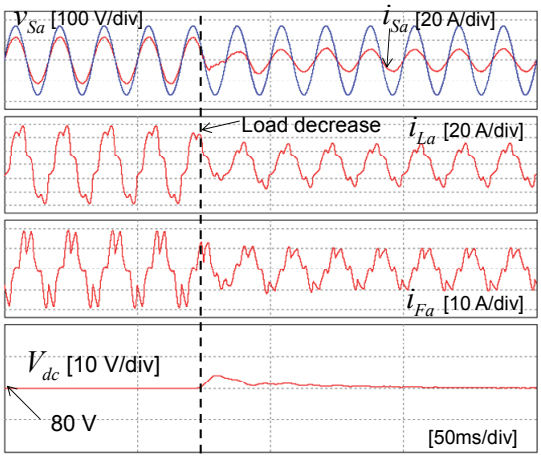

(b)

Fig. 10. Dynamic response of the proposed SHPF under load changing (a) load increase, (b) load decrease

Table 2. Comparisons of different active power filter topologies

	Pure shunt APF	Typical SHPF	Proposed SHPF
I_{APF}[A]	6.5	5.6	2.9
V_{dc}[V]	350	80	80
S_{APF}[VA]	2344	475	246
S_{APF} / S_{Load}	46.8 %	9.5 %	4.92%

Table 2 shows a comparison for operation current, voltage, and power of the active filter in a pure shunt APF [5], a typical SHPF [6], and the proposed SHPF under a 5 kVA load condition. From Table 2, it can be observed that the active filter in the proposed SHPF demands lower current, voltage, and power compared to both the pure shunt APF and the typical SHPF. Therefore, the proposed SHPF scheme can be regarded as a cost-effective solution for harmonic current and reactive power compensation.

5. Experimental Verifications

To experimentally verify the effectiveness of the proposed scheme, we built an experimental system in the laboratory with the same parameters used in the simulation, as shown in Fig. 11. The proposed SHPF was composed of a passive part consisting of an *LC* filter and an active part. The active part of the proposed SHPF was implemented with three IGBT modules (FMG2G50US60 from Fairchild). The control strategy was realized by a 32-bit floating-point DSP (TMS320F28335 of Texas Instruments). The supply voltage was generated by a programmable AC power source (Chroma 61704). The THD values of the load voltage and the supply current were measured using a power analyzer (HIOKI 3193).

In the experimental tests, due to the unavailability of inductive loads in the laboratory, only a three-phase diode rectifier was used in the load side. In this case, the THD and PF of the load current were about 30.2% and 0.85, respectively. The steady-state performance of the proposed SHPF with the proposed control strategy is illustrated in Fig. 12. It can be seen that the supply current was effectively compensated to be sinusoidal and in-phase with the supply

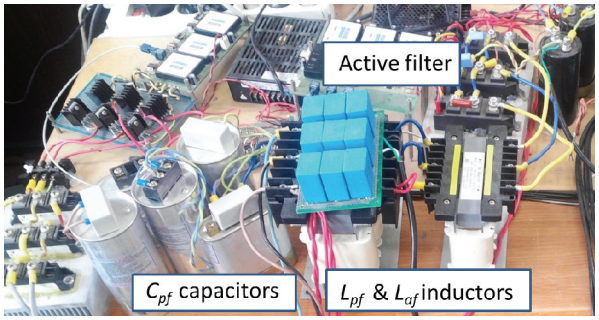

Fig. 11. Experimental system for the proposed SHPF

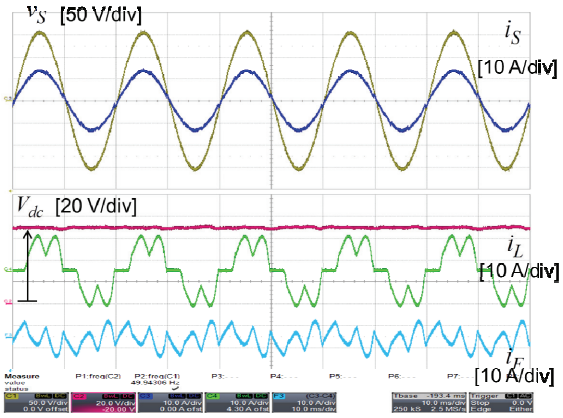

Fig. 12. Steady-state performance of the proposed SHPF

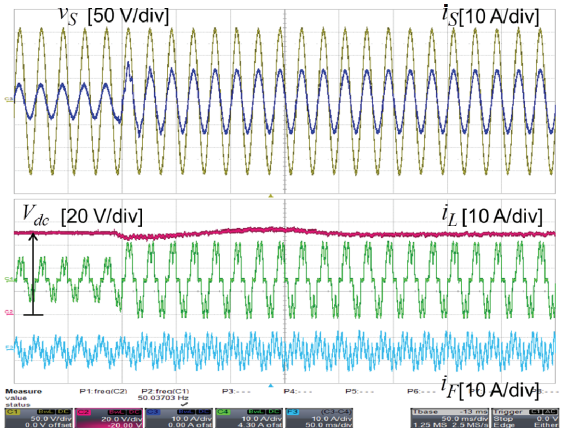

Fig. 13. Dynamic response of the proposed SHPF with increasing load

voltage even though the load current was highly distorted with poor PF. The THD and PF of the supply current after compensation were about 2.17% and 0.995, respectively. These experimental results completely verify the validity of the proposed SHPF topology and control strategy.

The dynamic response of the proposed SHPF with respect to load change is illustrated in Fig. 13. It is obvious that the supply current is quickly compensated to be sinusoidal within three fundamental cycles after a sudden load change. The supply current is always compensated to be sinusoidal and in-phase with the supply voltage, regardless of the load current condition. The proposed SHPF scheme provides good steady-state performance as well as robust and fast dynamic response.

6. Conclusions

This paper proposes a new control strategy for a novel SHPF to simultaneously compensate the harmonic current and the reactive power. The design of the passive components and the current controller for the SHPF were presented in detail. The effectiveness of the proposed topology is verified through simulated and experimental results: the supply current after compensation is almost sinusoidal with a very low THD of about 2.17% and is in-phase with the supply voltage with an almost unity power factor, regardless of the distorted load current condition. The proposed SHPF provides good steady-state performance and fast dynamic performance. Moreover, the proposed SHPF has a lower power rating requirement compared to pure shunt APF and typical SHPF topology. Thanks to its low-cost and high-performance qualities, the proposed SHPF topology is suitable to apply in high-voltage high-power applications.

Acknowledgment

This work was supported by the National Research Foundation of Korea Grant funded by the Korean Government (NRF-2010-0025483).

This work was supported by the National Research Foundation of Korea Grant funded by the Korean Government (NRF-2013R1A2A2A01016398).

References

[1] D. Rivas, L. Moran, J. W. Dixon and J. R. Espinoza "Improving passive filter compensation performance with active techniques", *IEEE Trans. Ind. Electron.*, vol. 50, no. 1, pp. 161-170 2003.

[2] W.-C. Lee, "Cost-Effective APF/UPS System with Seamless Mode Transfer", *Journal of Electrical Engineering & Technology,* vol. 10, no. 1, pp. 195-204, Jan. 2015.

[3] Y.-G. Jung, "Graphical Representation of the Instantaneous Compensation Power Flow for Single-Phase Active Power Filters," *Journal of Electrical Engineering & Technology,* vol. 8, no. 6, pp. 1380-1388, Nov. 2013.

[4] Hao Yi, Fang Zhuo, Yu Li, Yanjun Zhang, and Wenda Zhan, "Comparison Analysis of Resonant Controllers for Current Regulation of Selective Active Power Filter with Mixed Current Reference", *Journal of Power Electronics*, vol. 13, no. 5, pp. 861-876, Sep. 2013

[5] Q. N. Trinh; H. H. Lee, "An Advanced Current Control Strategy for Three-Phase Shunt Active Power Filters," *IEEE Trans. Ind. Electron.*, vol.60, no. 12, pp. 5400-5410, Dec. 2013.

[6] W. Tangtheerajaroonwong, T. Hatada, K. Wada, and H. Akagi, "Design and performance of a transformerless shunt hybrid filter integrated into a three-phase diode rectifier," *IEEE Trans. Power Electron*., vol. 22, no. 5, pp. 1882-1889, Sep. 2007.

[7] S. Rahmani, A. Hamadi, N. Mendalek, and K. Al-Haddad, "A new control technique for three-phase shunt hybrid power filter," *IEEE Trans. Ind. Electron*.,

vol. 56, no. 8, pp. 2904-2915, Aug. 2009.
[8] Rahmani, S.; Hamadi, A.; Al-Haddad, K., "A Lyapunov-Function-Based Control for a Three-Phase Shunt Hybrid Active Filter," *IEEE Trans. Ind. Electron.*, vol. 59, no. 3, pp. 1418,1429, March 2012.
[9] Corasaniti, V.F.; Barbieri, M.B.; Arnera, P.L.; Valla, M.I., "Hybrid Power Filter to Enhance Power Quality in a Medium-Voltage Distribution Net-work," *IEEE Trans. Ind. Electron.*, vol. 56, no. 8, pp. 2885-2893, Aug. 2009.
[10] Yan Li and Gang Li, "A Novel Hybrid Active Power Filter with a High-Voltage Rank", *Journal of Power Electronics*, vol. 13, no. 4, pp. 719-728, July 2013.
[11] MinhThuyen Chau, An Luo, Zhikang Shuai, Fujun Ma, Ning Xie, and Van Bao Chau, "Novel Control Method for a Hybrid Active Power Filter with Injection Circuit Using a Hybrid Fuzzy Controller", *Journal of Power Electronics*, vol. 12, no. 5, pp. 800-812, Sep. 2012.
[12] An Luo; Ci Tang; Zhi Kang Shuai; Wei Zhao; Fei Rong; Ke Zhou, "A Novel Three-Phase Hybrid Active Power Filter With a Series Resonance Circuit Tuned at the Fundamental Frequency," *Industrial Electronics, IEEE Transactions on*, vol. 56, no. 7, pp. 2431, 2440, July 2009.
[13] C.-S. Lam; M.-C. Wong; W.-H. Choi; X.-X. Cui; H.-M. Mei; J.-Z. Liu, "Design and Performance of an Adaptive Low-DC-Voltage-Controlled LC-Hybrid Active Power Filter With a Neutral Inductor in Three-Phase Four-Wire Power Systems," *IEEE Trans. Ind. Electron.*, vol. 61, no. 6, pp. 2635-2647, June 2014
[14] Rahmani, S.; Hamadi, A.; Al-Haddad, K.; Dessaint, L.A., "A Combination of Shunt Hybrid Power Filter and Thyristor-Controlled Reactor for Power Quality," *IEEE Trans. Ind. Electron.*, vol. 61, no. 5, pp. 2152-2164, May 2014.
[15] Q. N. Trinh; H. H. Lee, "Harmonic Current and Reactive Power Compensation with Novel Shunt Hybrid Power Filter", in Proc. *The 20th International Conference Electrical and Electronics Engineering*, 15-18, June, 2014, pp. 1-6.
[16] Q. N. Trinh and H. H. Lee, "An Advanced Repetitive Controller to Improve the Voltage Characteristics of Distributed Generation with Nonlinear Loads", *J. Power Electronics,* vol. 13, no. 3, pp. 409-418, May 2013.
[17] K. Zhang, Y. Kang, J. Xiong, and J. Chen, "Direct repetitive control of SPWM inverters for UPS purpose," *IEEE Trans. Power Electron*., vol. 18, no. 3, pp. 784-792, May 2003.

Hong-Hee Lee received his B.S., M.S., and Ph.D. in Electrical Engineering from Seoul National University, Seoul, Korea, in 1980, 1982, and 1990, respectively. From 1994 to 1995, he was a Visiting Professor at the Texas A&M University. He has been a Professor in the School of Electrical Engineering in the Department of Electrical Engineering, University of Ulsan, Ulsan, Korea since 1985. He is also the Director of the Network-based Automation Research Center (NARC), which is sponsored by the Ministry of Trade, Industry and Energy. His research interests include power electronics, network-based motor control, and renewable energy. Dr. Lee is a member of the Institute of Electrical and Electronics Engineers (IEEE), the Korean Institute of Power Electronics (KIPE), the Korean Institute of Electrical Engineers (KIEE), and the Institute of Control, Robotics and Systems (ICROS).

Quoc-Nam Trinh was born in Vietnam, in 1985. He received the B.S. degree from Ho Chi Minh City University of Technology, Vietnam, in 2008 and the Ph.D degree from University of Ulsan, Korea in 2014 both in Electrical Engineering. Currently, he is a postdoctoral research fellow at Energy Research Institute @ NTU, Nanyang Technological University, Singapore. His research interests are active power filters, harmonic compensation, distributed generation, and grid-connected inverters.